


Evaluation of Musculoskeletal and Pulmonary Bacterial Infections With [^{124}I]FIAU PET/CT

Steve Y. Cho, MD^{1,2}, Steven P. Rowe, MD, PhD¹ , Sanjay K. Jain, MD³,
Lew C. Schon, MD^{4,5}, Rex C. Yung, MD⁶, Tariq A. Nayfeh, MD, PhD⁷,
Clifton O. Bingham III, MD⁸, Catherine A. Foss, PhD¹,
Sridhar Nimmagadda, PhD¹ , and Martin G. Pomper, MD, PhD¹

Abstract

Purpose: Imaging is limited in the evaluation of bacterial infection. Direct imaging of in situ bacteria holds promise for noninvasive diagnosis. We investigated the ability of a bacterial thymidine kinase inhibitor ([^{124}I]FIAU) to image pulmonary and musculoskeletal infections.

Methods: Thirty-three patients were prospectively accrued: 16 with suspected musculoskeletal infection, 14 with suspected pulmonary infection, and 3 with known rheumatoid arthritis without infection. Thirty-one patients were imaged with [^{124}I]FIAU PET/CT and 28 with [^{18}F]FDG PET/CT. Patient histories were reviewed by an experienced clinician with subspecialty training in infectious diseases and were determined to be positive, equivocal, or negative for infection.

Results: Sensitivity, specificity, positive-predictive value, negative-predictive value, and accuracy of [^{124}I]FIAU PET/CT for diagnosing infection were estimated as 7.7% to 25.0%, 0.0%, 50%, 0.0%, and 20.0% to 71.4% for musculoskeletal infections and incalculable-100.0%, 51.7% to 72.7%, 0.0% to 50.0%, 100.0%, and 57.1% to 78.6% for pulmonary infections, respectively. The parameters for [^{18}F]FDG PET/CT were 75.0% to 92.3%, 0.0%, 23.1% to 92.3%, 0.0%, and 21.4% to 85.7%, respectively, for musculoskeletal infections and incalculable to 100.0%, 0.0%, 0.0% to 18.2%, incalculable, and 0.0% to 18.2% for pulmonary infections, respectively.

Conclusions: The high number of patients with equivocal clinical findings prevented definitive conclusions from being made regarding the diagnostic efficacy of [^{124}I]FIAU. Future studies using microbiology to rigorously define infection in patients and PET radiotracers optimized for image quality are needed.

Keywords

PET, infection, thymidine kinase, molecular imaging

¹ The Russell H. Morgan Department of Radiology and Radiological Science, Johns Hopkins University School of Medicine, Baltimore, MD, USA

² Department of Radiology, University of Wisconsin School of Medicine and Public Health, Madison, WI, USA

³ Division of Infectious Diseases, Department of Pediatrics, Johns Hopkins University School of Medicine, Baltimore, MD, USA

⁴ Department of Orthopedic Surgery, MedStar Union Memorial Hospital, Baltimore, MD, USA

⁵ Department of Orthopaedic Surgery, Johns Hopkins University School of Medicine, Baltimore, MD, USA

⁶ Division of Pulmonary Medicine and Critical Care, Department of Medicine, Johns Hopkins University School of Medicine, Baltimore, MD, USA

⁷ Metro Orthopedics and Sports Therapy, Potomac, MD, USA

⁸ Division of Rheumatology, Department of Medicine, Johns Hopkins University School of Medicine, Baltimore, MD, USA

Submitted: 24/01/2020. Revised: 22/05/2020. Accepted: 25/05/2020.

Corresponding Authors:

Steven P. Rowe and Martin G. Pomper, The Russell H. Morgan Department of Radiology and Radiological Science, Johns Hopkins University School of Medicine, Johns Hopkins Outpatient Center Room 3233, 601 N. Caroline St., Baltimore, MD 21287, USA.

Emails: srowe8@jhmi.edu; mpomper@jhmi.edu



Creative Commons Non Commercial CC BY-NC: This article is distributed under the terms of the Creative Commons Attribution-NonCommercial 4.0 License (<https://creativecommons.org/licenses/by-nc/4.0/>) which permits non-commercial use, reproduction and distribution of the work without further permission provided the original work is attributed as specified on the SAGE and Open Access pages (<https://us.sagepub.com/en-us/nam/open-access-at-sage>).

Introduction

In a number of clinical contexts, the definitive and noninvasive diagnosis of infection remains challenging. For example, areas of complex anatomy, such as the soft tissues and bony structures of the musculoskeletal system, can be difficult to accurately evaluate with current conventional imaging.¹⁻³ Further, both neoplastic and infections processes in the lungs can take on a mass-like morphology and may be difficult to distinguish using noninvasive methods.^{4,5} Uncertainty in these scenarios exists despite many imaging modalities available for the evaluation of patients with suspected infection,³ including plain film radiographs, computed tomography (CT), magnetic resonance imaging (MRI), single-photon nuclear medicine techniques (including ^{99m}Tc-methylene diphosphonate (MDP) bone scans, ⁶⁷Ga-citrate, ^{99m}Tc-labeled leukocytes, and ¹¹¹In-labeled leukocytes), and positron emission tomography (PET) with 2-deoxy-2-[¹⁸F]fluoro-D-glucose (FDG). The unifying characteristic of the multitude of imaging modalities currently in clinical practice is that none directly image the infecting bacterial organisms but instead image some aspects of the host response to the infection—this contributes to an intrinsic lack of specificity, as these host responses are not unique to bacterial infections. As a result, agents that directly image the presence of bacteria within infected tissues offer the potential of increasing specificity in imaging infection, correspondingly improving the guidance of appropriate therapy.⁶⁻⁹

Perhaps the most extensively studied examples of agents that directly image bacteria are the radiolabeled antibiotics such as ^{99m}Tc-ciprofloxacin, which has found some applicability in preclinical human trials at sites of potential infection that are otherwise difficult to evaluate with imaging.¹⁰⁻¹² However, specificity remains a concern, with uptake seen in both infections and sterile inflammatory processes.¹³ In addition to radiolabeled antibiotics, radiolabeled antimicrobial peptides have also been preclinically developed; for example, UBI,²⁹⁻⁴¹ derived from the endogenous antimicrobial peptide ubiquicidin, has shown promise in detecting active infection.¹⁴ However, questions remain about the ability of these compounds to discriminate different types of infections¹⁵ or to image pathogens with inaccessible membranes (such as those that are intracellular).¹⁶ At least partly as a result of these limitations, no agent that directly images bacteria in humans has become widely clinically available.

In the course of studying a bacterial-based cancer therapeutic agent, the compound 1-(2'-deoxy-2'-fluoro-β-D-arabinofuranosyl)-5-iodouracil (FIAU) was found to be a substrate for the native bacterial thymidine kinase (TK) and once phosphorylated by TK was trapped in the bacterial cells.¹⁷ A radiolabeled version of FIAU ([¹²⁵I]FIAU) was utilized for imaging bacterial infections in a mouse model.¹⁷ This suggested that a radiolabeled version of FIAU might also serve as a noninvasive means of directly imaging bacterial infections *in vivo* in humans. The initial human experience utilizing [¹²⁴I]FIAU in this context, reported by Diaz et al, appeared promising with

the successful imaging of 8 of 8 patients with confirmed musculoskeletal infections.¹⁸ However, a more recent effort at imaging suspected prosthetic joint infections suggested that the clinical utility of the radiotracer might be hampered by poor image quality and low specificity.¹⁹

In this study, we further expand upon these results by imaging a group of patients with [¹²⁴I]FIAU who were suspected to have musculoskeletal or pulmonary infections and patients with known rheumatoid arthritis (RA) with presumed sterile inflammatory changes in their joints.

Materials and Methods

General Methods

This study was approved by the institutional review boards of the Johns Hopkins Medical Institutions (Baltimore, Maryland) and Sinai Hospital (Baltimore, Maryland). A total of 33 patients were recruited for this study from these institutions and were categorized into 3 different cohorts based on their clinical presentations (see below). All patients signed written informed consent.

The first subset of patients consisted of 16 individuals presenting with clinical complaints suspicious for musculoskeletal infection. In addition to the standard clinical evaluation of these patients, including anatomic imaging (radiographs, CT scans, and MRI scans, as indicated) and laboratory and culture evaluation, 14 of 16 were imaged with FDG PET/CT and 14 of 16 were imaged with [¹²⁴I]FIAU PET/CT. One of the patients, after having been evaluated by the study team and accrued into the study, underwent an urgent surgical debridement of his distal upper extremity site of infection prior to either of the PET/CT examinations being performed, and he was excluded from further analysis; all other patients in this cohort were imaged with at least one of the PET radiotracers.

The second subset consisted of 14 patients presenting with pulmonary complaints and were found on plain film radiographs and/or CT imaging to have segmental or lobar lung consolidation or a cavitating mass-like lesion. Again, in addition to the standard-of-care workups in these patients including the above-noted imaging, laboratory analyses, and sputum and blood cultures, 11 of 14 patients were imaged with FDG PET/CT, and all 14 were imaged with [¹²⁴I]FIAU PET/CT.

Finally, 3 patients with known RA and mono- or oligoarticular pain were enrolled in the study. At the time of enrollment, these patients all had joint pain and/or swelling. Clinical suspicion for septic arthritis or another active infectious process was low, and this patient subset was intended to serve as a negative control group (ie, no significant [¹²⁴I]FIAU uptake was expected at the site(s) of their presumed sterile inflamed joint(s)).

Radiosynthesis and PET/CT Acquisition

The radiosynthesis of [¹²⁴I]FIAU was carried out as previously described according to good manufacturing practice (GMP) protocols (18) or was obtained from 3D Imaging.

FDG PET/CT scans were performed according to the standard clinical protocol in our department, with image acquisition beginning 1 hour after the injection of approximately 370 MBq (10 mCi) of FDG. For the [124 I]FIAU PET/CT acquisitions, patients were injected with 129.5 to 166.5 MBq (3.5-4.5 mCi) of the radiotracer (specific activity 27-35 Ci/ μ mol) intravenously administered 2 hours before imaging. Prior to, and after, undergoing imaging with [124 I]FIAU, thyroid blockade was performed with 200 mg of potassium iodide in saturated solution (SSKI). SSKI was initiated 24 hours before administration of [124 I]FIAU and was continued for 7 days after. All scans were acquired on a Discovery DRX PET/CT scanner (GE Healthcare) operating in 3D emission mode with CT-derived attenuation correction (120 kVp, 80 mA maximum [auto-adjusting]). Generally, whole-body acquisitions from the skull base through the mid-thigh were obtained for those patients being evaluated for potential pulmonary infections. For the suspected musculoskeletal infection and RA cohorts, the whole-body acquisitions were extended to include any extremity focus of suspected infection or inflammation. The acquisition consisted of 5 minutes per bed position, with each bed position covering 35 axial slices of 4.25-mm thickness; generally, at least 6 bed positions were required to complete the PET scan depending on patient height and the coverage length of any extremity that was imaged. The images of PET were reconstructed from the raw data using a standard clinical iterative reconstruction ordered subset expectation maximization algorithm.

Image Analysis

[124 I]FIAU and FDG PET, CT, and fused PET/CT images were exported to and reviewed on a Mirada Medical XD workstation (Mirada Medical). The images were reviewed by 2 nuclear medicine imaging specialists (S.P.R. and S.Y.C.), and a consensus determination was made as to whether uptake was positive (visually above blood pool activity) or negative (visually at or below blood pool activity). In those patients with positive uptake with either of the 2 radiotracers, the maximum standardized uptake values (SUVs) corrected for lean body mass of the lesions of interest were determined.

Clinical Truth Standard

A subspecialty trained infectious diseases physician (S.K.J.) reviewed all of the cases. That physician was provided with detailed anonymized histories of the patients' relevant clinical courses as well as any available laboratory values, culture results, surgical pathology results, and findings from conventional imaging modalities (including any clinically indicated radiographs, CT scans, MRI scans, and single-photon nuclear medicine procedures performed). He was blinded to the images and interpretations of the FDG and [124 I]FIAU PET/CT studies. Patients were categorized as positive, negative, or indeterminate for clinical infection based on the aggregate of the provided information.

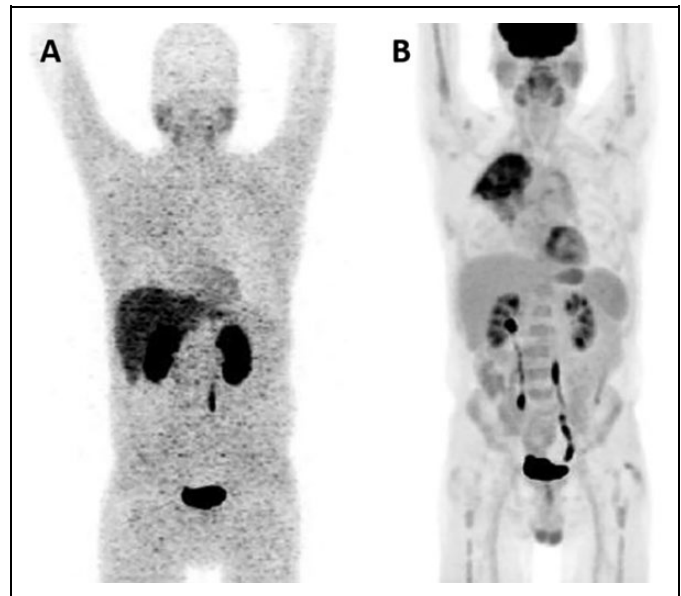


Figure 1. A, [124 I]FIAU positron emission tomography (PET) maximum intensity projection (MIP) from a patient with a suspected right upper lung infection demonstrating subtle asymmetric uptake of radiotracer at the site of suspected infection as well as the normal biodistribution of [124 I]FIAU with localization within the salivary glands, liver, kidneys, bladder, and blood pool. B, FDG PET MIP in the same patient with more obvious radiotracer uptake in the right upper lung.

The sensitivities, specificities, positive-predictive values (PPVs), and negative-predictive values (NPVs) of FDG and [124 I]FIAU PET/CT were calculated.

Results

General

Patient accrual occurred between November 2010 and April 2013. In total, 31 patients were imaged with [124 I]FIAU, and 27 had correlative FDG PET images. In all cases in which both scans were obtained, FDG PET was performed first. The median time between scans was 1.5 days, with a range from 1 to 21 days. Ten patients were on antibiotics at the time of initial imaging, with a median time on antibiotics of 19 days and a range from 1 to 160 days.

An example of a whole-body maximum intensity projection (MIP) of [124 I]FIAU is shown in Figure 1A; this image is from a patient with suspected pulmonary infection. The normal biodistribution of [124 I]FIAU, as demonstrated in this image, includes uptake in the salivary glands, blood pool, liver, spleen, stomach, kidneys, and bladder. The patient in Figure 1A also has faint radiotracer uptake in the right upper lung. For comparison, a whole-body MIP image from the corresponding FDG PET in the same patient is shown in Figure 1B and demonstrates the well-known biodistribution of FDG as well as uptake in the patient's known right upper lung pulmonary process.

Table 1. Imaging Findings and Retrospective Clinical Assessment.

Patient	Site of interest	Uptake on FDG PET/CT	Uptake on ¹²⁴ I-FIAU PET/CT	Clinical truth panel consensus
Suspected musculoskeletal infection				
1	Left hand	Negative ^a	Negative ^a	Positive
2	Right foot	Positive	Negative	Positive
3	Left shoulder (history of recent hemiarthroplasty for this joint)	NA	Negative	Indeterminate
4	Left foot	Positive	Negative	Indeterminate
5	Right hip (remote history of arthroplasty for this joint)	Positive	Negative	Indeterminate
6	Left foot	Positive	Negative	Indeterminate
7	Left hip (remote history of arthroplasty for this joint)	Positive	NA	Indeterminate
8	Right knee	Positive	Positive	Negative
9	Right great toe	Positive	Negative	Indeterminate
10	Left heel	Positive	Negative	Indeterminate
11	Left hip (remote history of arthroplasty for this joint)	Positive	Negative	Indeterminate
12	Left foot	Positive	Positive	Positive
13	Right foot	Positive	Negative	Indeterminate
14	Right sacroiliac joint	Positive	Negative	Indeterminate
15	Right sacroiliac joint	Positive	Negative	Positive
Suspected pulmonary infection				
16	Right lower lobe and left lower lobe	Positive	Negative	Negative
17	Right lower lobe and left lower lobe	Positive	Negative	Negative
18	Right upper lobe	Positive	Positive	Negative
19	Lingula	NA	Negative	Negative
20	Left upper lobe	Positive	Negative	Negative
21	Right upper lobe	Positive	Positive	Indeterminate
22	Right upper lobe	Positive	Positive	Indeterminate
23	Left lower lobe	Positive	Positive	Negative
24	Right lower lobe	Positive	Positive	Negative
25	Right upper lobe	NA	Positive	Indeterminate
26	Right upper lobe	Positive	Negative	Negative
27	Left lower lobe	NA	Negative	Negative
28	Left upper lobe	Positive	Negative	Negative
29	Right upper lobe	Positive	Negative	Negative
Rheumatoid arthritis				
30	Right ankle	Positive	Positive	Negative
31	Left knee	Positive	Negative	Negative
32	Bilateral shoulders, elbows, and knees	Positive	Negative	Negative

^aPatient had surgical debridement prior to imaging with either FDG or ¹²⁴I-FIAU.

Patients With Suspected Musculoskeletal Infections

Of those patients with suspected musculoskeletal infections, 4 were determined by our clinical truth panel to be definitively clinically infected, with 1 being deemed clinically noninfected, and 10 falling into an indeterminate category (Table 1). From this patient cohort, 2 of 14 patients had [¹²⁴I]FIAU uptake that was definitively higher than blood pool activity, while 12 of 14 were felt to be negative for significant uptake. [¹²⁴I]FIAU PET/CT successfully identified only 1 of 4 patients whose clinical course was consistent with infection. However, the single patient determined to be clinically noninfected also had a positive [¹²⁴I]FIAU PET/CT scan. These numbers equate to a sensitivity of 25.0%, specificity of 0.0%, a PPV of 50.0%, a NPV of 0.0%, and an overall accuracy of 20.0% when ignoring the indeterminate clinical cases. Table 2 includes these values if

the indeterminate clinical cases are categorized as either positive or negative.

For this same patient cohort, 13 of 14 patients had positive FDG PET/CT scans, while 1 patient was negative for abnormal FDG uptake. This equates to a sensitivity of 75.0%, specificity of 0.0%, PPV of 75.0%, NPV of 0.0%, and overall accuracy of 60.0%. The effects on these parameters of including the clinically indeterminate cases as either positive or negative are also shown in Table 2.

A representative patient from the cohort with suspected musculoskeletal infections is shown in Figure 2. This patient presented with an ulceration of the right heel with purulent drainage, and subsequent culture confirmed infection with *Staphylococcus aureus*. Figure 2A-C is notable for lack of focal [¹²⁴I]FIAU uptake, although Figure 2D-F demonstrates intense FDG uptake fusing to the right calcaneus and overlying soft tissues.

Table 2. Sensitivity, Specificity, PPV, NPV, and Overall Accuracy Ranges for [¹²⁴I]FIAU and FDG in Patients With Suspected Musculoskeletal Infections.

Radiotracer	Parameter	Indeterminate clinical cases ignored	Indeterminate clinical cases considered as positives	Indeterminate clinical cases considered as negatives
¹²⁴ I-FIAU	Sensitivity	25.0%	7.7%	25.0%
	Specificity	0.0%	0.0%	90.0%
	PPV	50.0%	50.0%	50.0%
	NPV	0.0%	0.0%	75.0%
	Overall Accuracy	20.0%	7.1%	71.4%
FDG	Sensitivity	75.0%	92.3%	75.0%
	Specificity	0.0%	0.0%	0.0%
	PPV	75.0%	92.3%	23.1%
	NPV	0.0%	0.0%	0.0%
	Overall Accuracy	60.0%	85.7%	21.4%

Abbreviations: PPV, positive-predictive value; NPV, negative-predictive value.

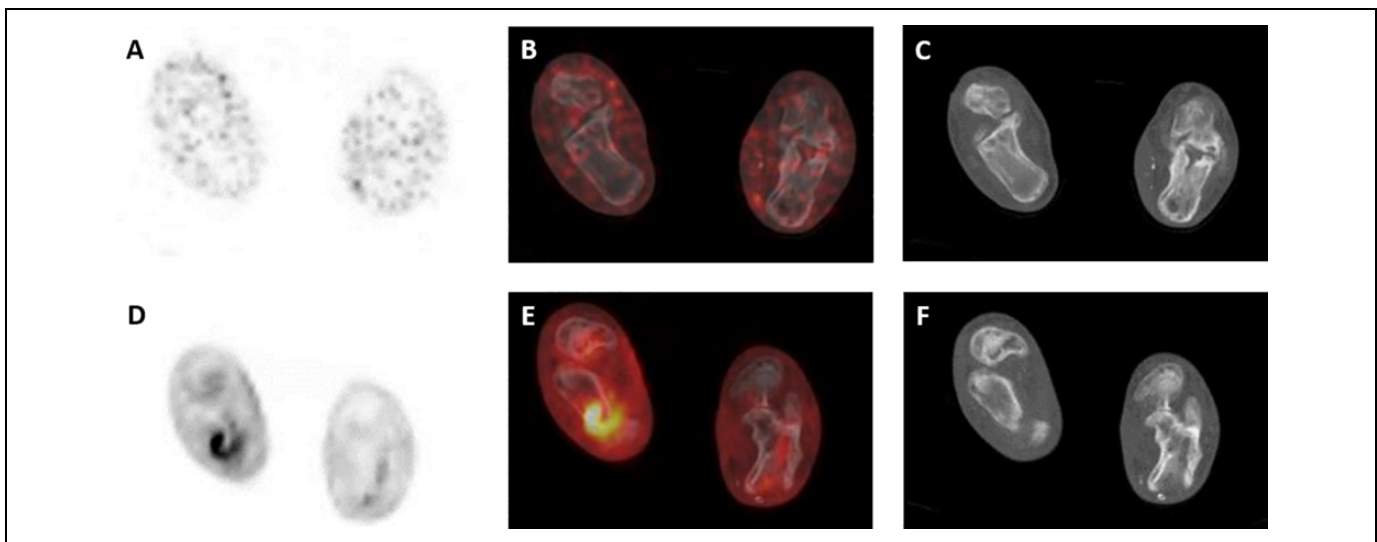


Figure 2. A, [¹²⁴I]FIAU positron emission tomography (PET), (B) [¹²⁴I]FIAU PET/computed tomography (CT), and (C) CT axial images through the feet at the level of the calcanei in a patient presenting with purulent drainage from an ulcer in the right foot and culture-proven *Staphylococcus aureus* infection. No appreciable focal [¹²⁴I]FIAU uptake is present. D, FDG PET, (E) FDG PET/CT, and (F) CT axial images through the same level as (A-C). Intense radiotracer uptake is noted fusing to the right calcaneus and the overlying soft tissues.

Patients With Suspected Lung Infections

None of the 14 patients with suspected lung infections were determined by our clinical truth panel to be definitively infected, 3 were felt to be indeterminate, and 11 were thought not to be infected. Among these patients, 6 were observed to have [¹²⁴I]FIAU uptake above blood pool activity, and 8 were judged to have no significant [¹²⁴I]FIAU uptake. [¹²⁴I]FIAU PET/CT was positive in all 3 clinically indeterminate patients as well as in 3 considered negative for infection. Ignoring the clinically indeterminate patients, the sensitivity of [¹²⁴I]FIAU PET/CT was not calculable, while the specificity was 72.7%, PPV was 0.0%, NPV was 100.0%, and overall accuracy was 72.7%. These values, as well as the same parameters with the indeterminate clinical

cases considered either positive or negative, are summarized in Table 3.

For these patients, the FDG PET/CT results are as follows (Table 3). All 11 of the patients scanned with FDG were positive for uptake. In this patient cohort, ignoring the indeterminate clinical cases, the sensitivity of FDG PET/CT was not calculable, specificity was 0.0%, PPV was 0.0%, NPV was not calculable, and overall accuracy was 0.0%.

Figure 3 illustrates representative imaging findings from a patient with rapid progression of a right upper lobe cavitory lesion, suspicious on conventional imaging for an infectious process but without definitive positive culture and considered indeterminate clinically. Figure 3A-C shows the cavitory lesion with moderate associated peripheral [¹²⁴I]FIAU uptake.

Table 3. Sensitivity, Specificity, PPV, NPV, and Overall Accuracy Ranges for [¹²⁴I]FIAU and FDG in Patients With Suspected Pulmonary Infections.

Radiotracer	Parameter	Indeterminate clinical cases ignored	Indeterminate clinical cases considered as positives	Indeterminate clinical cases considered as negatives
¹²⁴ I-FIAU	Sensitivity	NA	100.0%	NA
	Specificity	72.7%	72.7%	57.1%
	PPV	0.0%	50.0%	0.0%
	NPV	100.0%	100.0%	100.0%
	Overall Accuracy	72.7%	78.6%	57.1%
¹⁸ F-FDG	Sensitivity	NA	100.0%	NA
	Specificity	0.0%	0.0%	0.0%
	PPV	0.0%	18.2%	0.0%
	NPV	NA	NA	NA
	Overall Accuracy	0.0%	18.2%	0.0%

Abbreviations: PPV, positive-predictive value; NA, not available; NPV, negative-predictive value.

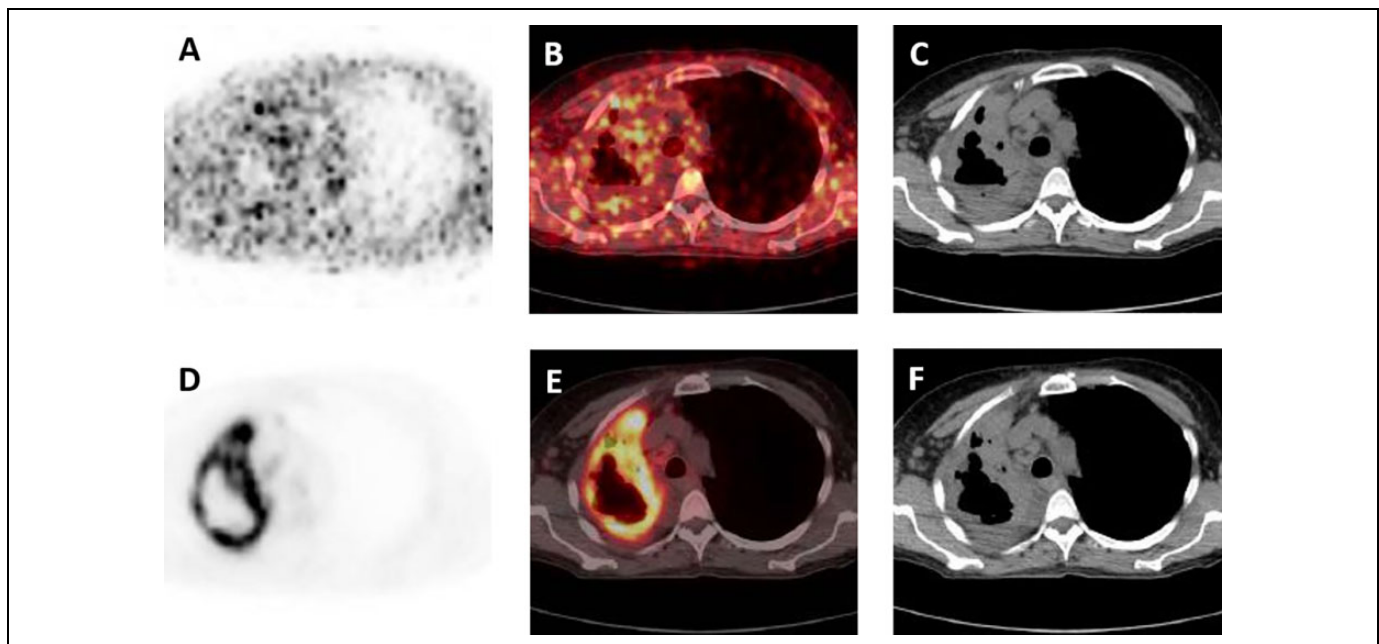


Figure 3. A, [¹²⁴I]FIAU positron emission tomography (PET), (B) [¹²⁴I]FIAU PET/computed tomography (CT), and (C) CT axial images of the chest in a patient with a rapidly progressing right upper lobe cavitory lesion, thought to represent infection on conventional imaging. Moderate [¹²⁴I]FIAU uptake is present in the periphery of the lesion. D, FDG PET, (E) FDG PET/CT, and (F) CT axial images through the same level as (A-C), with evidence of intense radiotracer uptake fusing to the periphery of the right upper lobe cavitory lesion. Definitive culture diagnosis of infection was not obtained in this patient, and retrospective clinical analysis categorized this patient as indeterminate for infection.

Figure 3D-F demonstrates the corresponding FDG findings with intense radiotracer uptake fusing to the periphery of the cavitory lesion.

Patients With Known Rheumatoid Arthritis

Only 3 patients with mono- or oligoarticular RA and without clinical suspicion for infection were imaged as part of this study. Two of the 3 patients had no appreciable uptake on [¹²⁴I]FIAU PET/CT, although 1 of the 3 patients had focal [¹²⁴I]FIAU uptake fusing to the periarticular tissues of the right great toe. As none of these patients were deemed to be

clinically infected, sensitivity and PPV cannot be calculated. [¹²⁴I]FIAU PET/CT specificity in this patient group was 66.7%, NPV was 100%, and overall accuracy was 66.7%.

The FDG PET/CT findings in these patients were as expected. Although generally articular and periarticular FDG uptake was mild to moderate, nonetheless all 3 patients did have focal FDG positivity corresponding to sites of their clinical symptoms.

As a corollary to the findings shown in Figure 2, Figure 4 shows representative images from the [¹²⁴I]FIAU PET/CT and FDG PET/CT studies for a patient from the RA cohort and a painful left great toe. Despite no clinical evidence to suggest

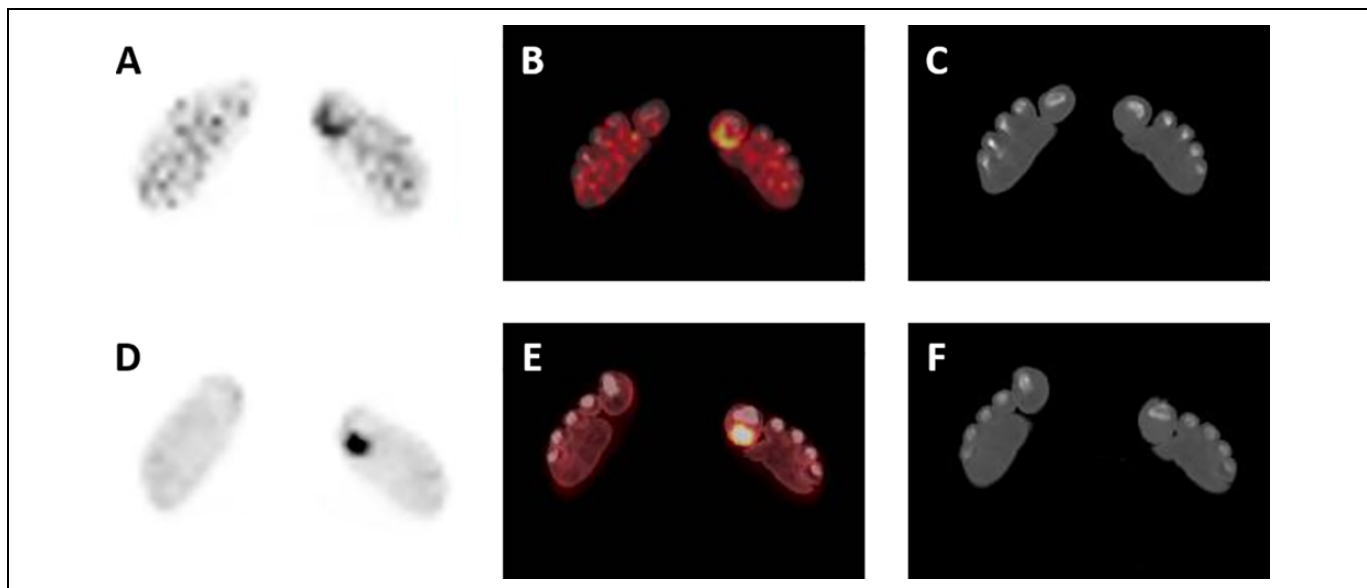


Figure 4. A, [^{124}I]FIAU positron emission tomography (PET), (B) [^{124}I]FIAU PET/computed tomography (CT), and (C) CT axial images through the distal feet of a patient with known rheumatoid arthritis and no clinical suspicion of infection. Moderate [^{124}I]FIAU uptake can be seen in the plantar soft tissues of the left great toe. D, FDG PET, (E) FDG PET/CT, and (F) CT axial images through the same level as (A-C), with intense radiotracer uptake also fusing to the plantar soft tissues of the left great toe.

this patient was having septic arthritis, focal [^{124}I]FIAU uptake was noted at the site of pain in the plantar soft tissues of the right great toe (Figure 4A-C).

Discussion

[^{124}I]FIAU represents a PET radiotracer that was developed for the evaluation of patients with suspected bacterial infections. We had proposed that the biological mechanism of [^{124}I]FIAU function, that is, high-affinity binding to bacterial thymidine kinase with subsequent phosphorylation and trapping of the compound inside bacterial cells¹⁷ would allow specific and direct imaging of in situ bacterial infection and consequent differentiation of bacterial infection from aseptic inflammation and neoplasia. Unfortunately, the results of this study do not support a clear role for this radiotracer in the routine evaluation of infection in human subjects.

In both of the primary clinical contexts examined (suspected musculoskeletal infection and suspected pulmonary infection), [^{124}I]FIAU PET/CT was neither adequately sensitive nor specific to allow for the confident identification of active bacterial infection. Adding to the specificity concerns, [^{124}I]FIAU PET/CT uptake was noted in 1 of the 3 patients with known RA imaged as negative controls. The findings in the musculoskeletal cohort in the study are in stark contrast to the previously reported work in a similar patient group with the same radiotracer,¹⁸ although they are in concordance with the more recent disappointing findings in patients with suspected prosthetic joint infections.¹⁹ The discrepancy in findings between this study and that reported in the study by Diaz et al¹⁸ may arise from a number of factors, although the foremost difference between the 2 was in how the patients were selected (ie, this

study was intended to investigate a broader array of patients in a more real-world setting with multiple referring clinicians from more than one hospital, as opposed to the more controlled setting of Diaz et al¹⁸ in which highly selected patients with suspected musculoskeletal infections planned for surgical debridement were imaged).

A number of profound limitations played a role in the results of this trial. In general, patient accrual for this study was exceedingly difficult, particularly in regard to imaging patients who had not previously been treated with one or more courses of antibiotics (Table 4). The practice patterns at our institutions are to start antibiotics early in any patient with a suspected infection, even without objective evidence such as a fever or elevated white blood cell count. As a result, we were only able to image a small number of antibiotic treatment-naïve patients. The confounding effect on our results was potentially 2-fold: (1) The bacterial density in patients who may have been actively infected would have been lowered by antibiotic treatment, preventing adequate localization of [^{124}I]FIAU at sites of infection, and (2) the efforts to determine clinical truth retrospectively and definitively identify those patients with infection was hampered, leading to a large number of patients being classified as indeterminate for infection. Our negative control cohort with rheumatoid arthritis was also limited in that only clinical evaluation was utilized to rule out other etiologies for their symptoms. Of note, FDG PET/CT also showed suboptimal performance in accurately predicting active bacterial infection, although this was primarily a function of poor specificity.

The radiotracer itself also introduced limitations to this study. The low injected doses necessitated by the long physical and effective half-life of [^{124}I]FIAU as well as the physical properties of ^{124}I that lead to a preponderance of nonpositron

Table 4. Demographic and Clinical Information of the Patients in This Study.

Patient	Age	Gender	Site of interest	Prior antibiotic therapy
Suspected musculoskeletal infection				
1	40	M	Left hand	Vancomycin, Zosyn, Ciprofloxacin, Doxycycline
2	68	F	Right foot	Vancomycin, Zosyn
3	61	F	Left shoulder (history of recent hemiarthroplasty for this joint)	Vancomycin
4	59	M	Left foot	Cefazolin, clindamycin
5	67	M	Right hip (remote history of arthroplasty for this joint)	Doxycycline, rifampin
6	44	M	Left foot	Keflex
7	72	F	Left hip (remote history of arthroplasty for this joint)	Ciprofloxacin
8	59	F	Right knee	Sulfamethoxazole, mupirocin, ciprofloxacin
9	51	M	Right great toe	None
10	81	F	Left heel	None
11	51	M	Left hip (remote history of arthroplasty for this joint)	None
12	56	F	Left foot	Vancomycin
13	46	M	Right foot	None
14	58	M	Right sacroiliac joint	Ciprofloxacin, moxifloxacin
15	61	F	Right sacroiliac joint	Vancomycin, oxacillin
Suspected pulmonary infection				
16	72	F	Right lower lobe and left lower lobe	None
17	58	F	Right lower lobe and left lower lobe	None
18	60	M	Right upper lobe	None
19	78	F	Lingula	Vancomycin, zosyn
20	58	M	Left upper lobe	Cefepime, azithromycin
21	59	F	Right upper lobe	Levofloxacin, azithromycin, ceftriaxone, vancomycin, piperacillin, tazobactam
22	63	M	Right upper lobe	Avelox, ceftriaxone, augmentin, azithromycin
23	77	M	Left lower lobe	Bactrim, augmentin
24	69	M	Right lower lobe	Levofloxacin
25	60	F	Right upper lobe	None
26	79	M	Right upper lobe	None
27	75	M	Left lower lobe	None
28	64	M	Right upper lobe	None
29	83	M	Right upper lobe	Bactrim
Rheumatoid arthritis				
30	32	F	Right ankle	None
31	62	F	Left knee	None
32	60	M	Bilateral shoulders, elbows, and knees	None

emission decay,²⁰ significantly impaired image quality, and hindered definitive interpretation of the [¹²⁴I]FIAU PET/CT findings. Newer thymidine kinase-binding small molecules with more ideal radionuclides (eg, a number of ¹⁸F-labeled arabinofuranosyl nucleosides have been reported^{21,22}) offer the promise of addressing these limitations in image quality.

However, our experience would suggest that simply improving image quality will not be enough to validate the use of direct bacterial imaging agents for noninvasive identification of bacterial infections. Intensive engagement with frontline clinicians (emergency department physicians, internal medicine doctors, and infectious diseases specialists) to recruit patients for any follow-up studies in this field is necessary. We underestimated the importance of buy-in from many of

these stakeholders, contributing to an incredibly high rate of clinically indeterminate patients being enrolled in the study. As such, we recommend that the results of this study not be interpreted at face value as indicating a failure of the idea of direct bacterial imaging with [¹²⁴I]FIAU but rather as a cautionary tale as to the difficulties in carrying out research of this kind and the need to enlist study team members from multiple sources within the medical community.

Conclusions

Within the significant limits of this study, [¹²⁴I]FIAU PET/CT neither sensitively nor specifically identified active bacterial infection in the pulmonary or musculoskeletal systems. Further

effort is required to design and plan effective studies of this type and to identify PET radiotracers capable of reliably directly imaging bacteria to realize the promise of PET in infection imaging.

Acknowledgments

The authors thank EB009367 for financial support. The author thank Akimosa Jeffrey-Kwanisai for clinical trial coordination.


Declaration of Conflicting Interests


The authors declared no potential conflicts of interest with respect to the research, authorship, and/or publication of this article.

Funding

The authors disclosed receipt of the following financial support for the research, authorship, and/or publication of this article: authors received financial support from the National Institutes of Health (EB009367).

ORCID iDs

Steven P. Rowe  <https://orcid.org/0000-0003-2897-4694>

Sridhar Nimmagadda  <https://orcid.org/0000-0002-6413-7191>

Reference

- Turecki MB, Taljanovic MS, Stubbs AY, et al. Imaging of musculoskeletal soft tissue infections. *Skeletal Radiol.* 2010;39(10):957–971.
- Pattamaspong N, Sivasomboon C, Settakorn J, Pruksakorn D, Mutarak M. Pitfalls in imaging of musculoskeletal infections. *Semin Musculoskelet Radiol.* 2014;18(1):86–100.
- Rowe SP, Cho SY. The role of PET in the evaluation of musculoskeletal infections. *Semin Musculoskelet Radiol.* 2014;18(2):166–174.
- Woodring JH, Fried AM. Significance of wall thickness in solitary cavities of the lung: a follow-up study. *AJR Am J Roentgenol.* 1983;140(3):473–474.
- Odev K, Guler I, Altinok T, Pekcan S, Batur A, Ozbiner H. Cystic and cavitary lung lesions in children: radiologic findings with pathologic correlation. *J Clin Imaging Sci.* 2013;3:60.
- Jain SK. The promise of molecular imaging in the study and treatment of infectious diseases. *Mol Imaging Biol.* 2017;19(3):341–347.
- Naqvi SAR, Roohi S, Iqbal A, Sherazi TA, Zahoor AF, Imran M. Ciprofloxacin: from infection therapy to molecular imaging. *Mol Biol Rep.* 2018;45(5):1457–1468.
- Ankrah AO, Klein HC, Elsinga PH. New imaging tracers for the infected diabetic foot (nuclear and optical imaging). *Curr Pharm Des.* 2018;24(12):1287–1303.
- Arvieux C, Common H. New diagnostic tools for prosthetic joint infection. *Orthop Traumatol Surg Res.* 2019;105(1S):S23–S30.
- Yapar Z, Kibar M, Yapar AF, Togrul E, Kayaselcuk U, Sarpel Y. The efficacy of technetium-99 m ciprofloxacin (Infecton) imaging in suspected orthopaedic infection: a comparison with sequential bone/gallium imaging. *Eur J Nucl Med.* 2001;28(7):822–830.
- Singh B, Mittal BR, Bhattacharya A, Aggarwal A, Nagi ON, Singh AK. Technetium-99 m ciprofloxacin imaging in the diagnosis of postsurgical bony infection and evaluation of the response to antibiotic therapy: a case report. *J Orthop Surg (Hong Kong).* 2005;13(2):190–194.
- Sierra JM, Rodriguez-Puig D, Soriano A, Mensa J, Piera C, Vila J. Accumulation of 99mTc-ciprofloxacin in *Staphylococcus aureus* and *Pseudomonas aeruginosa*. *Antimicrob Agents Chemother.* 2008;52(7):2691–2692.
- Sarda L, Cremieux AC, Lebellec Y, et al. Inability of 99mTc-ciprofloxacin scintigraphy to discriminate between septic and sterile osteoarticular diseases. *J Nucl Med.* 2003;44(6):920–926.
- Akhtar MS, Qaisar A, Irfanullah J, et al. Antimicrobial peptide 99mTc-ubiquicidin 29-41 as human infection-imaging agent: clinical trial. *J Nucl Med.* 2005;46(4):567–573.
- Welling MM, Lupetti A, Balter HS, et al. 99mTc-labeled antimicrobial peptides for detection of bacterial and *Candida albicans* infections. *J Nucl Med.* 2001;42(5):788–794.
- Akhtar MS, Imran MB, Nadeem MA, Shahid A. Antimicrobial peptides as infection imaging agents: better than radiolabeled antibiotics. *Int J Pept.* 2012;2012:965238.
- Bettegowda C, Foss CA, Cheong I, et al. Imaging bacterial infections with radiolabeled 1-(2'-deoxy-2'-fluoro-beta-D-arabinofuranosyl)-5-iodouracil. *Proc Natl Acad Sci U S A.* 2005;102(4):1145–1150.
- Diaz LA Jr., Foss CA, Thornton K, et al. Imaging of musculoskeletal bacterial infections by [124I]FIAU-PET/CT. *PLoS One.* 2007;2(10):e1007.
- Zhang XM, Zhang HH, McLeroth P, et al. [(124I)]FIAU: Human dosimetry and infection imaging in patients with suspected prosthetic joint infection. *Nucl Med Biol.* 2016;43(5):273–279.
- Pentlow KS, Graham MC, Lambrecht RM, Cheung NK, Larson SM. Quantitative imaging of I-124 using positron emission tomography with applications to radioimmunodiagnosis and radioimmunotherapy. *Med Phys.* 1991;18(3):357–366.
- Mangner TJ, Klecker RW, Anderson L, Shields AF. Synthesis of 2'-deoxy-2'-[18F]fluoro-beta-D-arabinofuranosyl nucleosides, [18F]FAU, [18F]FMAU, [18F]FBAU and [18F]FIAU, as potential PET agents for imaging cellular proliferation. Synthesis of [18F]labelled FAU, FMAU, FBAU, FIAU. *Nucl Med Biol.* 2003;30(3):215–224.
- Rajamani S, Kuszpit K, Scarff JM, et al. Bioengineering of bacterial pathogens for noninvasive imaging and in vivo evaluation of therapeutics. *Sci Rep.* 2018;8(1):12618.